20 February 2012 Volume 100 Number 8

AIP | Applied Physics Letters

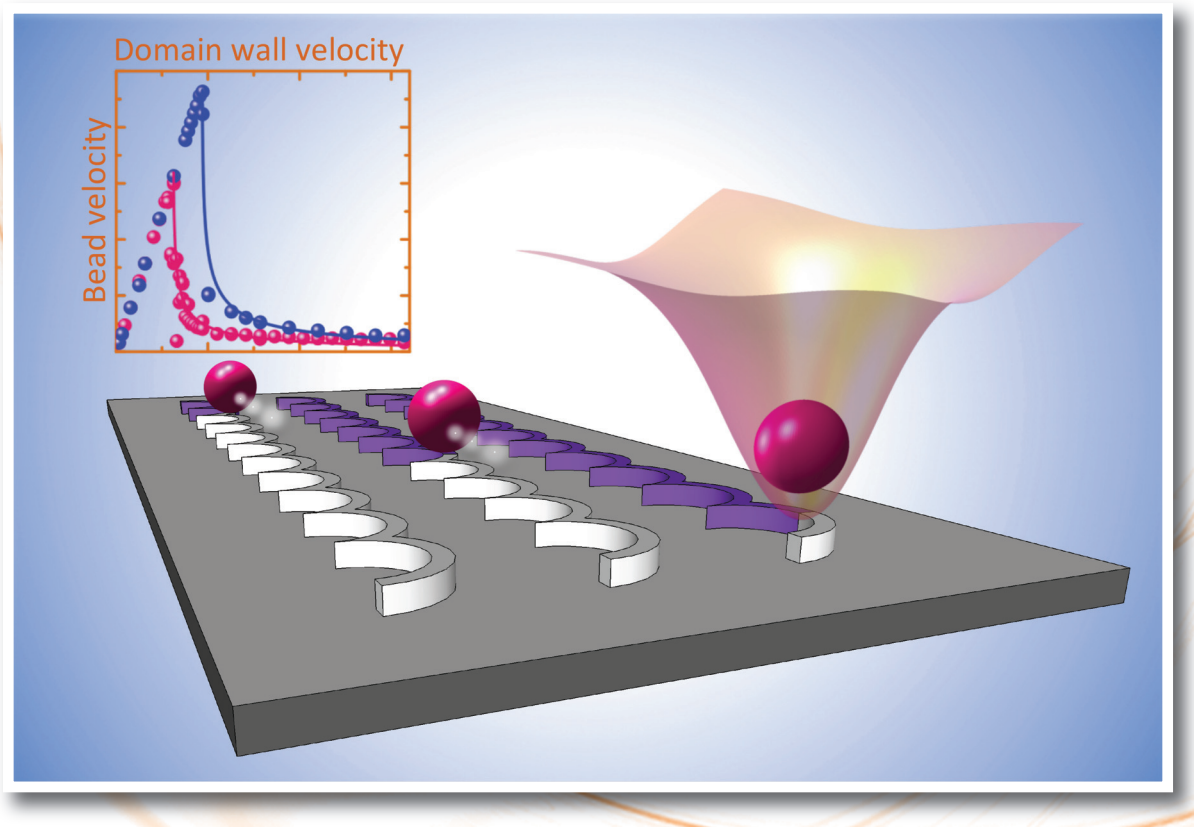

50th Anniversary

apl.aip.org

Dynamics of superparamagnetic microbead transport along magnetic nanotracks by magnetic domain walls

Elizabeth Rapoport and Geoffrey S. D. Beach[a)]
Department of Materials Science and Engineering, Massachusetts Institute of Technology, Cambridge, Massachusetts 02139, USA

(Received 28 September 2011; accepted 19 November 2011; published online 21 February 2012)

The dynamics of fluid-borne superparamagnetic bead transport by field-driven domain walls in submicrometer ferromagnetic tracks is studied experimentally together with numerical and analytical modeling. Experiments show that nanotrack-guided domain walls can propel individual trapped beads through an aqueous medium at speeds approaching 1000 μm/s, 10 to 100 times faster than through any previously demonstrated mechanism. © *2012 American Institute of Physics*. [doi:10.1063/1.3684972]

Substantial efforts have sought to exploit surface-functionalized superparamagnetic (SPM) microbeads for nanoscale control of cells or biomolecules in lab-on-chip devices.[1–14] Microscale electromagnets[1,4,5] and arrays of soft magnetic microstructures[2,3,7–13] have previously been used to transport microbead ensembles[1,3–5,7] and even individual beads[2,8–11] across the surface of a chip. Recently, it has been shown that the strong, localized stray field[15] from domain walls (DWs) in submicrometer ferromagnetic tracks can trap individual SPM beads with forces up to hundreds of pN.[4,8,11,14] As DWs can be readily driven along a track by a magnetic field[16–18] or spin-polarized electric current,[19,20] they can serve as mobile magnetic traps for single bead transport along a predefined path.

While microbead transport has been demonstrated in several nanotrack architectures, the dynamics of that transport has not been well explored. Recently, micromagnetic and analytical modeling[14] suggested that DWs could transport nanosized beads at speeds up to several mm/s through a fluid. Here, we examine the dynamical interactions between nanotrack-guided DWs and SPM beads in a viscous fluid. Continuous coupled transport can be sustained up to a critical velocity that depends on the ratio of the bead-DW magnetostatic binding force to the viscous drag on the bead.[14] Sustained transport speeds approaching 1000 μm/s are achieved using curvilinear track structures in which the DW speeds can be precisely controlled. Moreover, DWs traveling beyond the critical speed for coupled transport remain capable of displacing a bead, and rapid trains of fast DWs can propel a bead quasicontinuously along a track.

Fig. 1(a) summarizes the forces involved in DW-mediated bead transport through a viscous fluid. The DW stray field generates an attractive magnetostatic potential that binds the bead and DW together. As the Zeeman force from an external field drives the DW along a track, the magnetostatic interaction generates a force, F_{int}, that pulls the bead forward with the wall. Viscous drag from the host fluid resists bead motion, and in dynamic equilibrium, the bead is displaced from the DW center by an amount that increases the faster the pair move. The maximum speed for coupled transport is thus set by the maximum longitudinal restoring force, F_{bind}, that the magnetostatic potential can exert on the bead.

We have calculated F_{bind} as a function of bead size and track width over an experimentally realizable range. DW magnetization profiles were generated micromagnetically[21] and used to compute the DW stray field, $\mathbf{B}(\mathbf{r})$, via the scalar potential. The magnetostatic energy of a proximate SPM

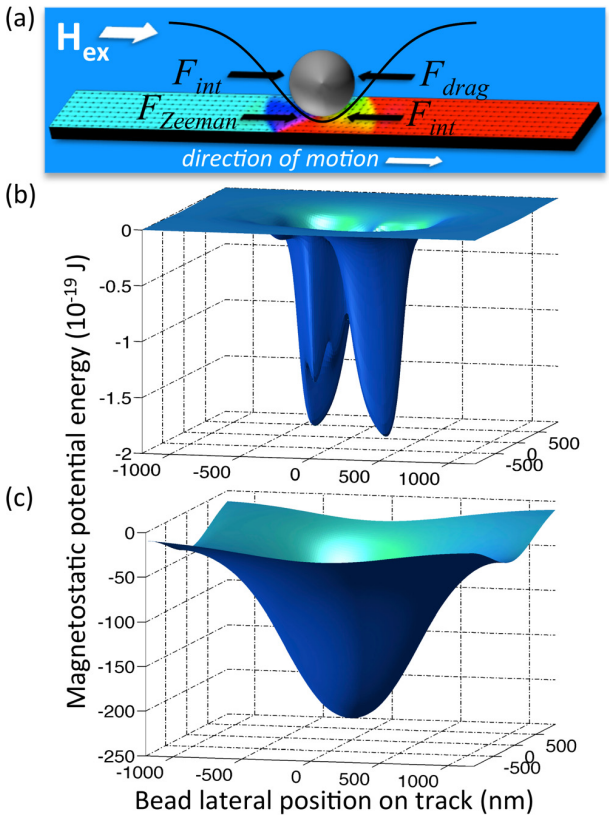

FIG. 1. (Color online) (a) Micromagnetically computed domain wall structure in a 400 nm wide × 40 nm thick $Ni_{80}Fe_{20}$ (Permalloy) track, with schematic of trapped bead and relevant forces during translation in a fluid. Magnetostatic potential energy versus lateral position is shown for a bead at the track surface with radius (b) 50 nm and (c) 1000 nm.

[a)]Author to whom correspondence should be addressed. Electronic mail: gbeach@mit.edu.

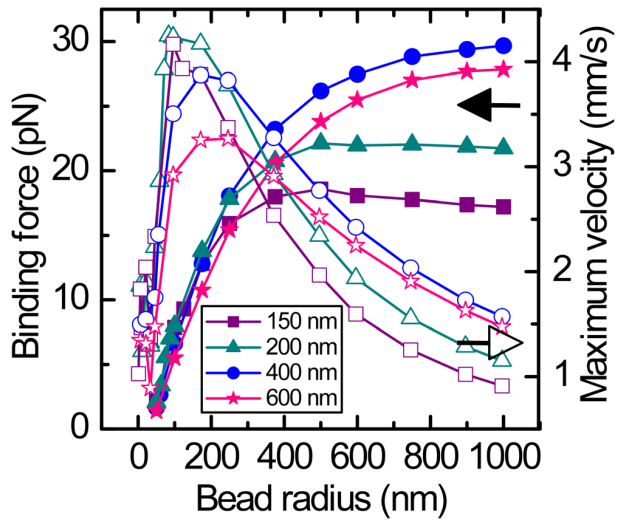

FIG. 2. (Color online) Calculated longitudinal magnetostatic binding force (solid symbols) and maximum coupled transport velocity (open symbols) versus bead radius for several track widths.

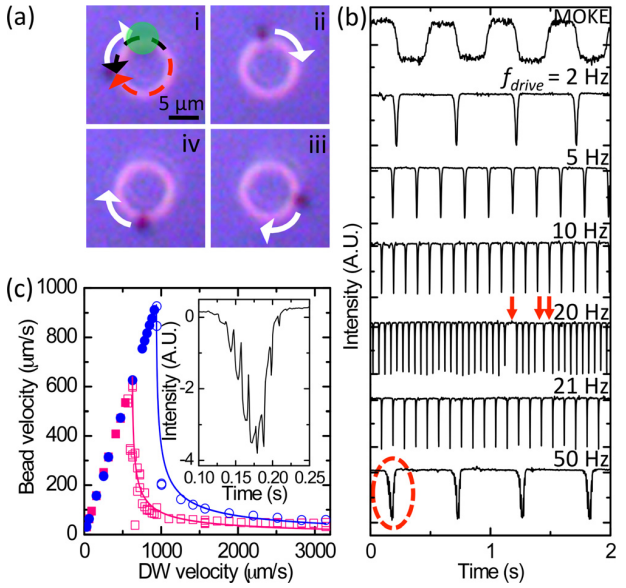

FIG. 3. (Color online) (a) i-iv: Sequential snapshots of a 1 μm diameter SPM bead driven around a 10 μm outer diameter $Ni_{80}Fe_{20}$ track by a 1 Hz clockwise rotating magnetic field. Domain orientation shown schematically in image (i). (b) MOKE signal (top trace) and optical reflectivity traces after bead capture for several drive frequencies. (c) Bead velocity versus DW velocity for two representative beads. Solid symbols indicate continuous transport regime and open symbols indicate stepwise transport. (c, inset) Zoom of the circled intensity dip in (b) showing progressive oscillatory stepping of the bead through the laser spot by each passing DW.

bead was then estimated by integrating the dipolar energy density $-\mathbf{M}\cdot\mathbf{B}$ over the bead volume, assuming bead magnetization $\mathbf{M}=\chi\mathbf{B}$. The volume susceptibility χ was taken as 800 kA m^{-1} T^{-1}, appropriate for the commercial microbeads in the experiments below.[6] Figs. 1(b) and 1(c) show potential landscapes for beads near the vortex DW[22] in the 400 nm wide, 40 nm thick $Ni_{80}Fe_{20}$ track in Fig. 1(a). The potential landscape for the 50 nm radius bead [Fig. 1(b)] follows the local DW stray field profile and exhibits several local minima. By contrast, a 1 μm radius bead near the same DW [Fig. 1(c)] yields a deep, nearly parabolic well, as the local field profile is averaged over the bead volume.

Calculations were repeated for beads with radius R spanning 50 nm to 1 μm, near tracks of several widths [Fig. 2]. F_{bind}, computed as the maximum longitudinal gradient of each potential, increases with R up to $R\sim400$ nm, then saturates as the stray field falls off with distance from the track. Following Ref. 14, maximum coupled transport speeds, v_{max}, were estimated by equating F_{bind} with viscous drag, assuming Stokes form $F_{drag}=-6\pi\eta Rv$ with the viscosity, η, of water (10^{-3} Pa s). As seen in Fig. 2, v_{max} increases with R until F_{bind} plateaus, then falls off as $\sim1/R$ as viscous drag continues to increase. Over a wide range of R, transport speeds in the mm/s range are predicted.

We have experimentally characterized the dynamics of SPM bead transport through an aqueous medium using DWs confined to circular ferromagnetic tracks. In this geometry, a strong in-plane magnetic field generates two circumferential domains separated by DWs lying along the field axis.[23] These DWs can then be repositioned or continuously driven around the track simply by rotating the field axis. Arrays of 800 nm wide, 40 nm thick, 10 μm outer diameter $Ni_{80}Fe_{20}$ tracks were fabricated on a Si wafer by electron beam lithography and sputter deposition. After initializing the tracks into the bi-domain state, a dilute suspension of 1 μm diameter SPM beads in phosphate buffered saline was placed on the wafer surface.

The sequential snapshots in Fig. 3(a) show a single trapped bead driven around a track by a 1 Hz rotating field. The bead continuously followed the field axis with a direction and speed consistent with the sense and rate of field rotation, respectively. The CCD frame rate was sufficient to monitor bead motion up to a drive frequency, f_{drive}, of several Hz. At higher speeds, beads were tracked using a probe laser focused to a $\sim$2 μm spot through the microscope objective. The probe spot was positioned at the track perimeter [Fig. 2(a)], where the reflected intensity was monitored in time. Bead traversal through the spot was accompanied by a momentary reflectivity dip. The laser probe also enabled direct detection of DW motion, via the longitudinal magneto-optical Kerr effect (MOKE), upon insertion of a polarizer in the reflected beam path.[24,25]

A MOKE signal trace acquired on the track in Fig. 3(a) under application of a 220 Oe, 2 Hz rotating field prior to bead capture is shown in Fig. 3(b). Each step in the trace represents a switch in the direction of tangential magnetization, due to passage of alternately head-to-head and tail-to-tail DWs. After bead capture, periodic reflectivity dips synchronous with DW circulation appeared [Fig. 3(b)], marking continuous bead transport as confirmed in simultaneous video imaging. The dip frequency tracked f_{drive} up to a limit of 19 Hz, but at $f_{drive}=20$ Hz, dips were occasionally absent, indicating intermittent bead dropping by one DW and subsequent capture and carry by the other. For $f_{drive}=21$ Hz, dropping and re-capture became regular with each revolution, evidenced by reflectivity dips at precisely half f_{drive}. At still higher f_{drive}, the dip frequency fell precipitously, but regular bead circulation was sustained.

Average bead circulation velocity, v_{bead}, versus DW velocity, v_{DW}, is plotted for two representative beads in

Fig. 3(c). For f_{drive} such that v_{DW} is below v_{max}, beads are transported by a single DW at DW velocity. Measurements for more than a dozen nominally identical beads showed similar behavior, with v_{max} ranging from $\sim$600 μm/s to $\sim$1000 μm/s. Bead-to-bead variations in v_{max} are attributed to distributions in bead size and magnetic content. These speeds are $\sim$10–100 times higher than have been reported for any other bead transport system,[1–13] and in reasonable agreement with the predictions in Fig. 2.

Video imaging at high f_{drive} showed continuous bead circulation in the direction of DW motion, but at a much lower rate. This motion suggests that the rapidly circulating DWs continually "knocked" the bead forward each time they passed. The laser-probe technique employed here permits detection of sub-100 nm transient bead displacements with high time resolution, providing evidence for this fast DW driven transport mechanism. Stepwise motion is visible in the high-f_{drive} reflectivity traces [Fig. 3(c), inset], which exhibit oscillations at $2f_{drive}$, commensurate with circulation of the two DWs. Upon entering the laser spot, forward (backward) bead displacement manifests as a decrease (increase) in reflected intensity; this correspondence is reversed as the bead emerges from the other side of the spot. From the trace in the inset in Fig. 3(c), each passing DW evidently pulls the bead abruptly back as it approaches from behind, then carries it forward until viscous drag separates it from the DW. A rapid train of DWs can thus propel a bead along a track even if their speed exceeds v_{max}.

Stepwise motion for $v_{DW} > v_{max}$ was modeled analytically by computing the bead displacement induced by a truncated harmonic potential (stiffness k, full width 2Δ) passing at a speed v_{DW}, assuming an overdamped linear viscous response, $F_{drag} = -bv_{bead}$. The bead dwell time in the DW potential falls with increasing v_{DW}, and for $v_{DW} \gg v_{max}$, the DW carries the bead a distance $\sim\Delta v_{max}/v_{DW}$ before the two separate. This simple model qualitatively reproduces the data in Fig. 3(c).

Finally, Fig. 4 shows a curvilinear track architecture in which fast transport over an extended distance can be sustained. Bead transport has been previously demonstrated along zig-zag magnetic tracks with DWs either pinned at each vertex[8] or stepped from vertex to vertex by applied field pulses,[9] with speeds limited to several tens of μm/s as the bead diffused from one local trap to another. By contrast, in the present geometry, beads translate synchronously with DWs at a well-defined speed. A rotating field drives DWs progressively along the track in tandem, moving them from one segment to the next with each half cycle. Translation speeds up to 150 μm/s were sustained as the bead was shuttled back and forth more than 200 times with no missteps, for a total travel distance of several cm. At higher speeds, the bead was intermittently trapped at the segment junctions, but junction optimization should enable translational speeds approaching the limit $2v_{max}/\pi$ suggested by geometrical considerations.

DW-mediated transport of individual SPM beads was observed at speeds approaching 1000 μm/s, and calculations suggest even higher speeds are possible in optimized geometries. DWs traveling faster than the limit for coupled transport remain capable of displacing a bead, and rapid trains of fast DWs can drive bead translation along arbitrary track geometries. The high speeds reported here open up the possibility of high-throughput microbead-based on-chip devices for sorting and sensing applications. Moreover, as the critical speed for coupled transport depends sensitively on the hydrodynamic properties of the trapped bead, DWs could be used to probe bead size and bead-surface interactions, providing a mechanism for single-bead metrology in an integrated bead transport system.

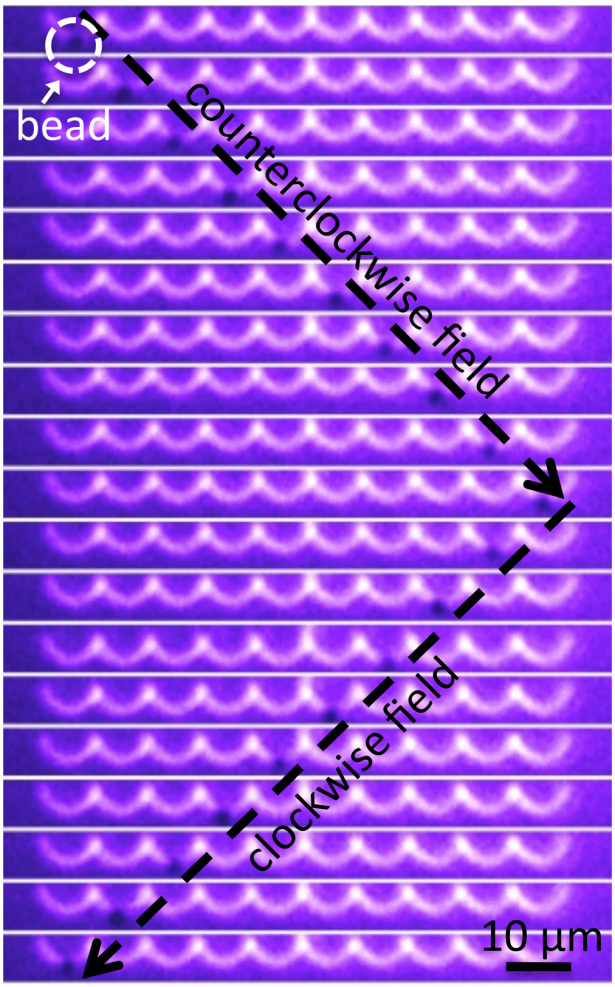

FIG. 4. (Color online) Sequential snapshots at 180° field rotation intervals show a trapped 1 μm diameter SPM bead driven along a ferromagnetic curvilinear track. Counterclockwise and clockwise field rotation results in motion to the right and the left, respectively.

Supported by NSF-MRSEC (DMR-0819762) and the MIT Deshpande Center. MIT CMSE, MIT NSL, and computational resources of A. Alexander-Katz are gratefully acknowledged.

[1]C. S. Lee, H. Lee, and R. M. Westervelt, Appl. Phys. Lett. **79**, 3308 (2001).
[2]K. Gunnarsson, P. Roy, S. Felton, J. Pihl, P. Svedindh, S. Berner, H. Lidbaum, and S. Oscarsson, Adv. Mater. **17**, 1730 (2005).
[3]B. Yellen, O. Hovorka, and G. Friedman, Proc. Natl. Acad. Sci. U.S.A. **102**, 8860 (2005).
[4]Q. Ramadan and C. Yu, Appl. Phys. Lett. **88**, 032501 (2006).
[5]C. Liu, L. Lagae, R. Wirix-Speetjens, and G. Borghs, J. Appl. Phys. **101**, 024913 (2007).

[6]R. Derks, A. Dietzel, R. Wimberger-Friedl, and M. Prins, Microfluid. Nanofluid. **3**, 141 (2007).
[7]J. Adams, U. Kim, and H. Soh, Proc. Natl. Acad. Sci. U.S.A. **105**, 18165 (2008).
[8]G. Vieira, T. Henighan, A. Chen, A. Hauser, F. Yang, J. Chalmers, and R. Sooryakumar, Phys. Rev. Lett. **103**, 128101 (2009).
[9]M. Donolato, P. Vavassori, M. Gobbi, M. Deryabina, M. F. Hansen, V. Metlushko, B. Ilic, M. Cantoni, D. Petti, S. Brivio *et al.*, Adv. Mater. **22**, 2706 (2010).
[10]G. Ruan, G. Vieira, T. Henighan, A. Chen, D. Thakur, R. Sooryakumar, and J. O. Winter, Nano Lett. **10**, 2220 (2010).
[11]T. Henighan, A. Chen, G. Vieira, A. J. Hauser, F. Y. Yang, J. J. Chalmers, and R. Sooryakumar, Biophys. J. **98**, 412 (2010).
[12]M. T. Bryan, K. H. Smith, M. E. Real, M. A. Bashir, P. W. Fry, P. Fischer, M.-Y. Im, T. Schrefl, D. A. Allwood, and J. W. Haycock, IEEE Magn. Lett. **1**, 1500104 (2010).
[13]L. Johansson, K. Gunnarsson, S. Bijelovic, K. Eriksson, A. Surpi, E. Göthelid, P. Svedlindh, and S. Oscarsson, Lab Chip **10**, 654 (2010).
[14]M. T. Bryan, J. Dean, T. Schrefl, F. E. Thompson, J. Haycock, and D. A. Allwood, Appl. Phys. Lett. **96**, 192503 (2010).
[15]M. Redjdal, J. Giusti, M. Ruane, and F. Humphrey, IEEE Trans. Magn. **39**, 2684 (2003).
[16]T. Ono, H. Miyajima, K. Shigeto, K. Mibu, N. Hosoito, and T. Shinjo, Science **284**, 468 (1999).
[17]D. Atkinson, D. Allwood, G. Xiong, M. Cooke, C. Faulkner, and R. Cowburn, Nature Mater. **2**, 85 (2003).
[18]D. Allwood, G. Xiong, C. Faulkner, D. Atkinson, D. Petit, and R. Cowburn, Science **309**, 1688 (2005).
[19]S. Parkin, M. Hayashi, and L. Thomas, Science **320**, 190 (2008).
[20]G. Beach, M. Tsoi, and J. Erskine, J. Magn. Magn. Mater. **320**, 1272 (2008).
[21]M. J. Donahue and D. G. Porter, *OOMMF User's Guide Version 1.0*, NIST, Gaithersburg, MD (1999).
[22]Y. Nakatani, A. Thiaville, and J. Miltat, J. Magn. Magn. Mater. **290–291**, 750 (2005).
[23]C. A. Ross, F. J. Castano, W. Jung, B. G. Ng, I. A. Colin, and D. Morecroft, J. Phys. D: Appl. Phys. **41**, 113002 (2008).
[24]D. Allwood, G. Xiong, M. Cooke, and R. Cowburn, J. Phys. D: Appl. Phys. **36**, 2175 (2003).
[25]G. Beach, C. Nistor, C. Knutson, M. Tsoi, and J. Erskine, Nature Mater. **4**, 741 (2005).